Int. J. Heat Mass Transfer. Vol. 7, pp. 1427–1443. Pergamon Press 1964. Printed in Great Britain

MEASUREMENTS OF THE GROWTH OF ELECTROLYTIC BUBBLES

J. P. GLAS* and J. W. WESTWATER
Division of Chemical Engineering, University of Illinois, Urbana, Illinois

(*Received* 10 *August* 1964)

Abstract—An experimental study of the growth of bubbles during electrolysis was carried out by means of high-speed motion picture photography through a microscope. The bubbles were H_2, O_2, Cl_2, and CO_2 on platinum, nickel, copper, and iron electrodes, at pressures from 1 to 2 atm, with controlled constant current densities from 0·01 to 0·12 A/cm^2. The asymptotic growth rates of the bubbles were found to agree with the theoretical predictions of either Scriven or Buehl and Westwater. Of 600 bubbles observed, none grew with a constant contact angle. A conclusion of significance to theoretical workers is that contact angle definitely is a very weak variable, at least in the range of 0 to about 100 degrees.

NOMENCLATURE

- C, dissolved gas concentration at r and t [g/cm^3];
- C_s, dissolved gas concentration at saturation [g/cm^3];
- C_∞, supersaturation in liquid [g/cm^3];
- C', constant for a liquid–gas system, $= D\mu/T$;
- D, mass diffusivity [cm^2/s];
- h, height of spherical segment [cm];
- I, current density [A/cm^2];
- K, empirical coefficient defined by equation (7);
- K_1, empirical coefficient defined by equation (8);
- K_2, empirical coefficient defined by equation (9);
- r, radial coordinate, in liquid phase [cm];
- R, bubble radius [cm];
- t, time [s];
- t_w, waiting time between bubbles [s];
- T, absolute temperature [°K];
- x, dummy variable [dimensionless].

Greek symbols

- α, contact angle measured through the liquid;
- β, growth coefficient defined by equation (2) [dimensionless];
- ϵ, $1 - (\rho_G/\rho_L)$ [dimensionless];
- μ, liquid viscosity [P];
- ρ_G, gas density [g/cm^3];
- ρ_L, liquid density [g/cm^3];
- Φ, function defined by equation (4) [dimensionless].

INTRODUCTION

BUBBLE GROWTH during electrolysis is one special case of a phase change. It is not as common as certain other phase changes such as condensation, evaporation, melting, or freezing, and therefore has been studied to a limited extent only. The study of bubble growth during electrolysis presumably can lead to improvements in commercial electrolytic processes. A further stimulus to the study is that electrical measurements can be made with great accuracy and with relative ease. Mathematically, bubble growth by mass transfer (e.g. electrolysis) is analogous to bubble growth by heat transfer (e.g. boiling liquid). The mathematical solution for one case can be converted to a solution for the other case by an interchange of appropriate dimensionless groups. Thus information concerning one phase change may contribute to knowledge of another.

The present study had the goal of achieving

* Research and Development Labs., E. I. Du Pont Co., Circleville, Ohio.

experimental data for the growth of bubbles during electrolysis. A previous study [1] had shown that the mathematical model used by Scriven [2] gave good first-order predictions for the growth of hydrogen bubbles on a platinum electrode with a constant electromotive force. The tests reported herein were much more extensive; including bubbles of H_2, O_2, Cl_2, and CO_2; on electrodes made of Pt, Ni, Fe, and Cu; using four sizes of electrodes; pressures from 1 to 2 atm, and current densities from 0·01 to 0·12 A/cm^2. The current density was held constant for each test. For many of the bubbles, the contact angle on the electrode was measured throughout their growth periods. Information concerning the contact angles was of particular interest because the Scriven model, and indeed all other models, assume radial symmetry or a contact angle of 90 degrees. Verification or repudiation of this assumption awaited experimentation.

PRIOR EXPERIMENTAL WORK

Coehn and Neumann [3] obtained break-off diameters for many electrolytic bubbles, but not the rate of growth. Kabanow and Frumkin [4] also obtained break-off diameters. Murakawa [5] showed that electrolytic bubbles grow at nucleation sites which were tiny surface scratches for O_2 and H_2 forming on Pt. The first study to include quantitative data for electrolytic bubble growth was that of Westerheide and Westwater [1]. This was carried out using high-speed motion picture photography through a microscope. In addition to the demonstration that the theoretical model of bubble growth as given by Scriven is promising, interesting observations were given concerning the coalescence of bubbles, the jumping of bubbles off the solid and then back on again, and the slip of the bubble contact at the solid surface. The photographic study also showed conclusively that electrolytic bubbles definitely form at nucleation sites, microscopic pits and scratches, on the electrode.

Experimental work on bubble growth during gas dissolution is related to bubble growth during electrolysis. The interested reader may consult the publications by Houghton *et al.* [6], Doremus [7], Buehl and Westwater [8]. Experimental work on bubble growth in boiling liquids is described elsewhere [9, 10].

STATE OF THEORETICAL KNOWLEDGE

Three regulating mechanisms are evident that may control the rate of growth of a bubble. One consists of mechanical forces such as pressure, surface tension, inertia, and viscous shear. This case was first considered by Rayleigh [11]. The force balance is not fruitful for the case of bubble growth during electrolysis. because insufficient information is available for solving the differential equation.

A second controlling mechanism is heat transfer. All phase changes are accompanied by a latent heat change, therefore, the heat balance should be considered in every case. However, for electrolytic bubbles the latent heat and sensible heat quantities seem to be small, and it is certainly convenient to assume they are zero. The equations for the force balance and the heat balance will not be repeated here. They are available in the literature [1, 2].

The third regulatory mechanism is the one of particular interest for electrolytic bubbles. This is mass diffusion. The electric field causes ions to move to the electrodes. Ions of a gas become neutralized, resulting in dissolved gas molecules. This gas diffuses through the liquid in response to concentration gradients. At a nucleation site the dissolved gas comes out of solution to form a growing bubble. The rate of diffusion of dissolved gas will control the rate of bubble growth.

The model which has been solved assumes that the bubble has spherical symmetry, is far away from any solid wall, and that the gas and liquid phases have constant density.

$$D\left[\frac{\partial^2 C}{\partial r^2}+\frac{2}{r}\frac{\partial C}{\partial r}\right]=\frac{\partial C}{\partial t}-\frac{\epsilon R^2}{r^2}\cdot\frac{\mathrm{d}R}{\mathrm{d}t}\cdot\frac{\partial C}{\partial r}. \qquad (1)$$

Equation (1) is a mass balance on the gas solute for a thin spherical shell of liquid surrounding the bubble.

Scriven [2] solved equation (1) by numerical means assuming uniform initial concentration. He assumed further that the liquid is of infinite extent and that the gas–liquid interface is at

equilibrium conditions. The resulting solution relating bubble radius to time is equation (2). This is an asymptotic solution which cannot be valid as time approaches zero.

$$R = 2\beta\sqrt{(Dt)} \tag{2}$$

The dimensionless coefficient β is related to two dimensionless groups ϵ and Φ as shown in equation (3).

$$\Phi = 2\beta^3 \exp(\beta^2 + 2\epsilon\beta^2) \int_{\beta}^{\infty} x^{-2} \exp(-x^2 - 2\epsilon\beta^3 x^{-1})\, dx \tag{3}$$

where

$$\Phi = \left(\frac{\rho_L}{\rho_G}\right)\left(\frac{C_\infty - C_s}{\rho_L - C_s}\right) \tag{4}$$

and

$$\epsilon = \frac{\rho_L - \rho_G}{\rho_L} \tag{5}$$

The numerical relationship between β and Φ, for the case of $\epsilon = 1$ is shown in Fig. 1.

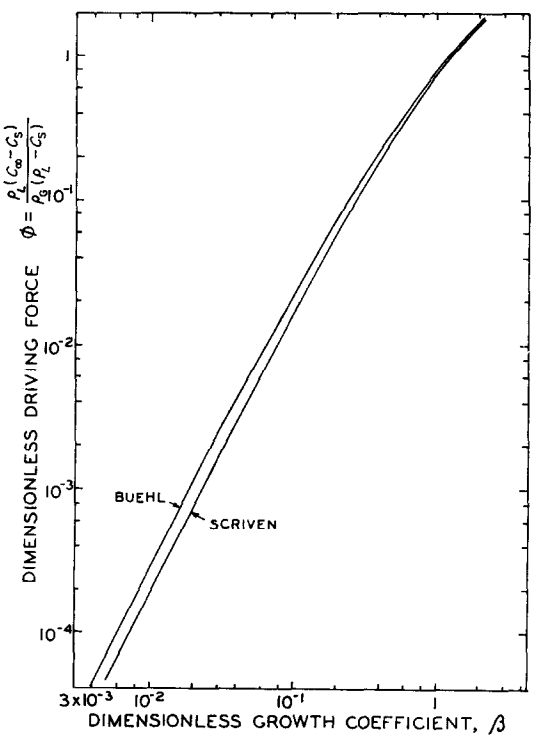

FIG. 1. Theoretical bubble growth coefficient, for atmospheric pressure. Scriven's values are for an isolated sphere. Buehl's values are for a sphere tangent to a plane.

Scriven's assumptions should be applicable to a hemisphere growing on a flat plane, provided the surface is frictionless. The assumptions are not applicable for a bubble on a wall with any contact angle other than 90°. Buehl and Westwater [8] have considered the interesting case of a spherical bubble tangent to a wall (contact angle of zero). The numerical solution results in the line shown also in Fig. 1.

Earlier workers solved equation (1) by making sufficient assumptions to permit direct integration. Epstein and Plesset [12] for example assumed that mass transfer by radial flow of the liquid did not occur. This made the last term in equation (1) equal to zero and led to an approximate solution which may be called the stationary case, equation (6).

$$\frac{dR}{d\theta} = \frac{D(C_\infty - C_s)}{\rho_G}\left[\frac{1}{R} + \frac{1}{\sqrt{(\pi Dt)}}\right] \tag{6}$$

Doremus [7] presents another stationary solution which seems to be a rougher approximation than equation (6). The data of Westerheide and Westwater for H_2 bubbles have been compared to equations (2) and (6). Equation (6) predicts growth rates 14–21 per cent lower than does equation (2). Therefore, the assumption of negligible convective transport is not a safe choice.

APPARATUS

The general features of the experimental equipment and procedure were the same as used earlier [1]. Improvements and modifications were made, and these are given below. A more detailed description is available [13]. Briefly, motion pictures were taken through a microscope of bubbles growing on a miniature electrode. Electrical meters gave the current and cell voltage; examination of the motion picture films gave bubble sizes and contact angle versus time. A schematic diagram of the apparatus is shown in Fig. 2.

Electrodes

The target electrode was the flat circular end of a small diameter wire. The wire was sealed in a capillary glass tube so that the tip only was exposed to the electrolyte. Electrolytic

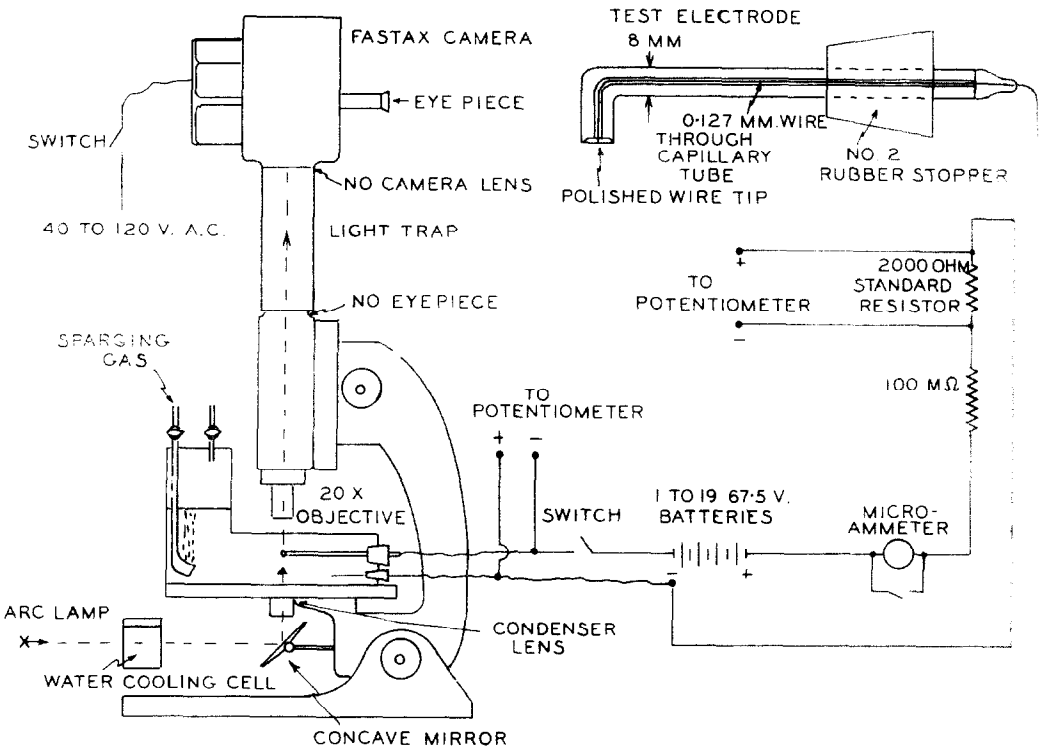

FIG. 2. Schematic diagram of the apparatus. Not to scale.

bubbles were frequently less than 0·05 mm in diameter at break-off, so the electrode size need not be much larger. Electrodes used were 0·127 mm wires of Pt, Ni, and Cu, 0·102 and 0·508 mm Ni, 0·228 mm Fe, and 0·254 mm Pt. The end surface was well polished with wet gamma alumina powder. This fact, coupled with the small size of the electrode, guaranteed a small population of bubbles at any time. For most runs, one bubble only was on the electrode.

The capillary tube was bent in an L shape. Rotation of the electrode by 90° made orientation of the flat surface possible either in the vertical or horizontal plane.

The other electrode was a length of 0·635 mm Pt wire formed into a loop of 38 mm diameter. This loop was in a horizontal plane, concentric with the target electrode. The electrodes were immersed in 60 or 200 cm^3 of electrolyte at room temperature (24–30°C) contained in a transparent plastic cell.

Test cell

Two designs of the test cell were used. One was the same as before [1] and this was suitable for H_2 and O_2, but not for CO_2 or Cl_2. The second design included a fritted-glass sparger so that CO_2 or Cl_2 from a gas tank could be bubbled through the liquid to maintain saturation conditions. Both cells had covers with a very small vent to the room to maintain the pressure at atmospheric. The test liquid remained saturated for short delay times even without a secondary source of gas, when H_2 or O_2 was used. But CO_2 and Cl_2 solutions rapidly became undersaturated during delays unless the sparger was kept in operation.

For H_2 and O_2 generation, the electrolytes were 0·1 N and 1·0 N H_2SO_4 solution in water. For Cl_2 the electrolyte was 1·0 N NaCl with 0·01 N NaOH. For CO_2 the electrolyte was 1·0 N sodium oxalate in 30 wt. % H_2SO_4 solution, as recommended by the National Bureau of Standards [14].

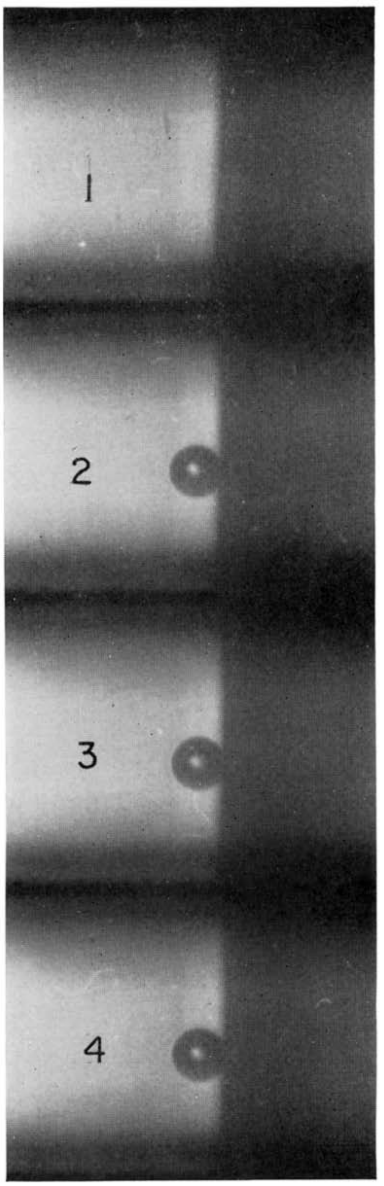

FIG. 3. Very rapid early growth of H_2 bubble on Ni in 1·0 N H_2SO_4 at 0·0344 A/cm². The measurements are in Fig. 7. 1 atm. Taken at 2520 frames/s. Bubbles are 185× actual size.

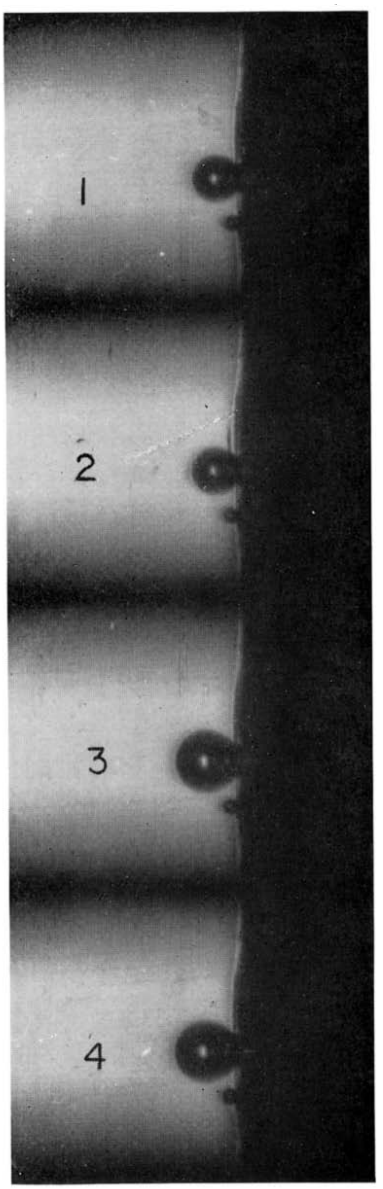

FIG. 5. Apparent step-growth, resulting from coalescence of normal bubble with one having very rapid early growth. H_2 on 0·127 mm Pt in 0·5 N $Na_2C_2O_4$ + 30 wt per cent H_2SO_4 at 0·0361 A/cm². 1 atm. Taken at 1440 frames/s. Bubbles are 197× actual size.

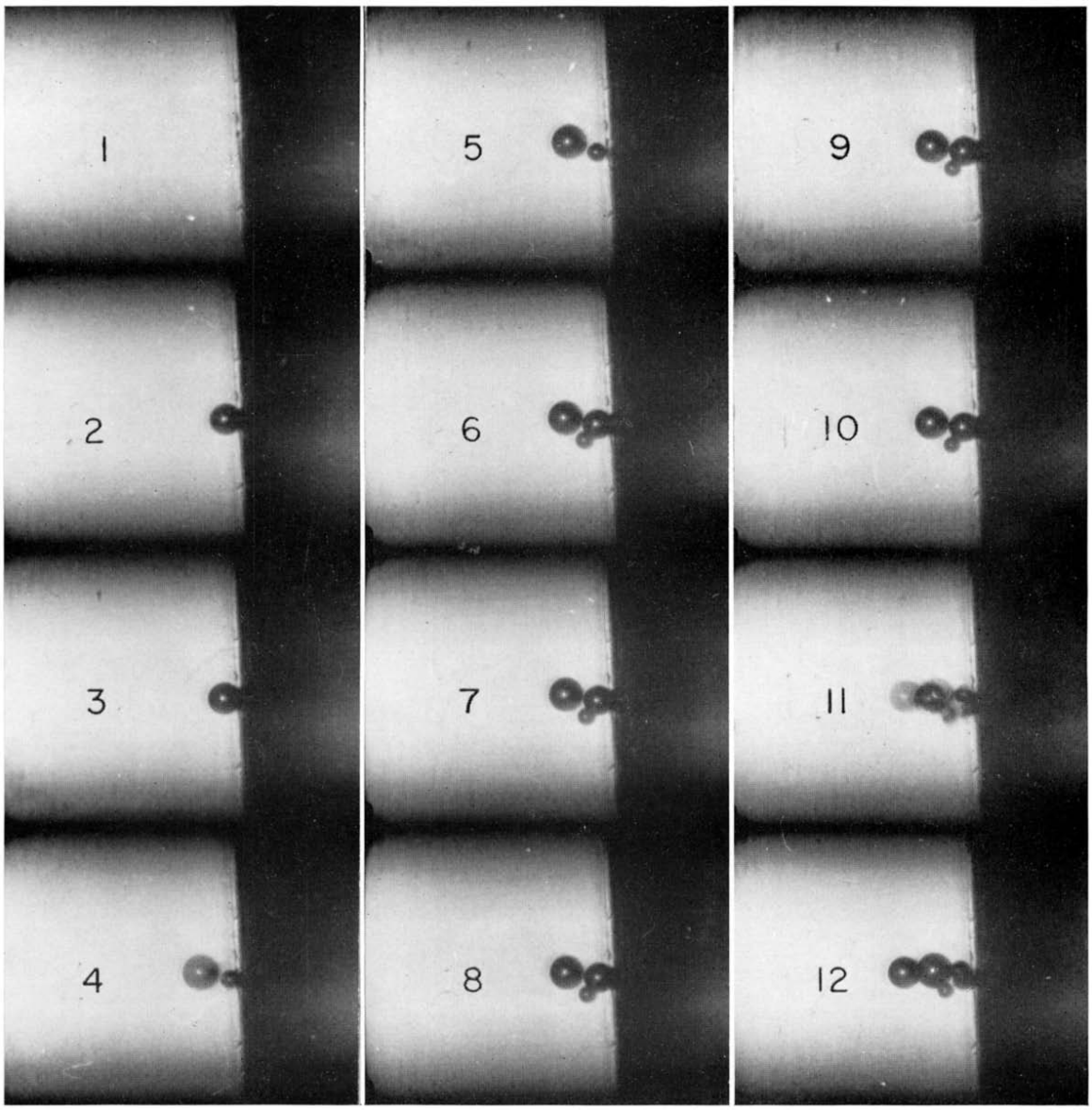

FIG. 4. Rapid-fire emission of CO_2 bubbles on 0·127 mm Pt in 1·0 N $Na_2C_2O_4$ + 30 wt per cent H_2SO_4 at 0·0362 A/cm^2.
Rough metal surface. 1 atm. Taken at 960 frames/s.
Bubbles are 180× actual size.

For certain tests with H_2 the test cell was sealed and pressurized with the test gas, and runs were carried out at a pressure of 1·5 to 2 atm.

Optics

The bubbles on the target electrode were illuminated with a carbon-arc lamp operated on direct currents between 5 and 20 A, according to the light requirements. The light beam passed through a condenser and a cooling cell. Illumination from below, using transmitted light, was used for profile views of the bubbles. The light then passed through a microscope and thence to the camera. For a plan view of bubbles, a metallographic microscope was used, and reflected light passed to the camera.

One lens only was in the target-to-camera path. This was a Leitz 20× achromatic objective with a 0·33 numerical aperture. This lens had a working distance of about 25 mm, therefore immersion of the lens in the electrolyte, as was done previously, was not necessary.

Two cameras were used for motion picture photography. Films at about 1500 frames/s were taken with a 16 mm Wollensak Fastax WF-14 camera using Kodak Tri-X and Double-X negative film. Timing marks on the edge of the film established the true framing rate. Films at 32 frames/s were taken with a 16 mm Paillard Bolex Rex camera using Double-X film. The framing rate was calibrated by photography of a running stop watch. Focusing was done directly on stationary film for the Fastax camera and on the ground glass viewer for the Bolex camera. True magnification was calibrated by photography of a micrometer slide. The enlargement on the negative was from 26 to 41 times real size. The value could be varied by changing the position of the lens and the camera.

Read-out of diameters, contact angles, and time was done on a Vanguard Motion Picture Analyzer. Bubble diameters on this machine were enlarged another 10×, or in general they were about 300 times actual size. The maximum and minimum of the diameter of the bubble were recorded for each frame examined. The bubbles were small and therefore had the shape of spherical segments. The contact angle therefor was computed readily from the two diameters. The accuracy of the analyser is supposedly within 0·025 mm on the viewing screen, or within 7×10^{-5} mm for the actual bubbles. Read-out data were recorded permanently on tapes by a Clary Numerical Data Printer upon push-button command.

The test cell and entire optical set-up were mounted on a vertical optical bench, isolated from building vibrations by rubber and felt pads.

Electrical system

An important difference existed between the electrical system used in the present study and the previous work [1]. It is not possible to have both constant current and constant e.m.f. during electrolysis. The prior study used a constant e.m.f. (to within 4 per cent for most of the bubbles) but the current varied by almost a factor of 2 during a run as a bubble grew on the electrode. For the present work a constant current was used.

Constant current was achieved by putting a 100 MΩ resistor in series with the test cell. The resistance of the test cell was negligible by comparison. This change required that the d.c. supply be increased from 3 to 1300 V. As a result the electrode current never varied as much as 1 per cent during a run. The current was determined by measurement of the voltage drop across a 2000 Ω standard resistor using a Rubicon potentiometer and a Shallcross electric galvanometer.

DISCUSSION OF RESULTS

The new data are available in detail [13]. A total of 600 bubbles were analysed. Figures 3, 4, and 5 are examples. The bubble images in the motion pictures are similar to those in the motion pictures made available for loan previously [15]. Sample photographs were published previously [1, 16]. The new data are used in Figs. 3 to 15 and in Fig. 17. The growth time for the bubbles studied varied from about 0·7 to 8 s. Bubble break-off occurred usually at bubble diameters of from about 0·05 to 0·20 mm.

Asymptotic growth

All the growth data were graphed as diameter

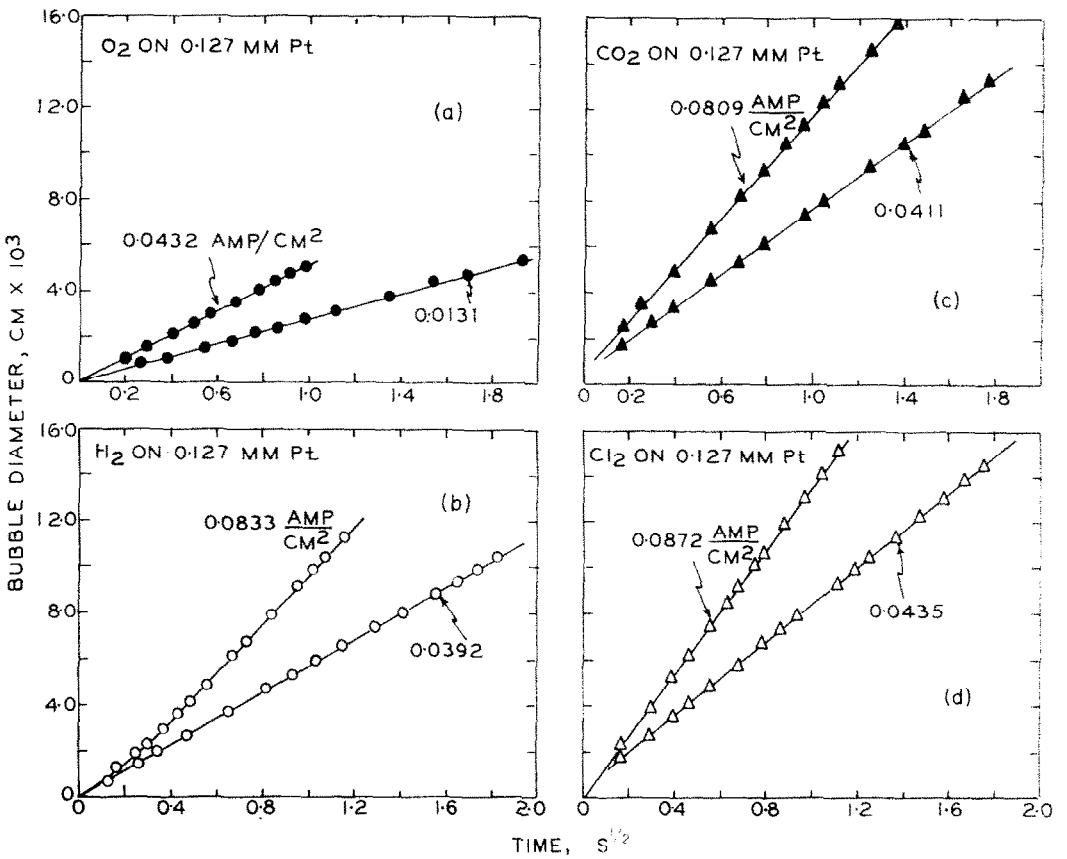

FIG. 6. Typical growth data for 8 bubbles at 1 atm. (a) O_2 in 1·0 N H_2SO_4. (b) H_2 in 1·0 N H_2SO_4. (c) CO_2 in 1·0 N $Na_2C_2O_4$ plus 30 per cent H_2SO_4. (d) Cl_2 in 1·0 N NaCl plus 0·01 N NaOH.

vs the square root of time. The great majority of the bubbles gave straight lines as shown in Figs. 6 and 7. This is in agreement with the R vs t functionality, equation (2), expected for asymptotic bubble growth. The slopes of the lines were used to obtain the experimental values of β, the growth coefficient. It is not possible yet to measure experimentally the supersaturation, C_∞, in the electrolyte near the electrode during bubble growth. However, this value can be computed from a measured value of β by using Fig. 1 and assuming one of the theoretical lines to be correct. Thus, we may expect that when measurements of C_∞ are devised, it will become possible to choose between the theoretical models relating β and Φ. The computed supersaturations, expressed as C_∞/C_s, ranged from 1·54 to 19·9 for H_2, 1·36 to 15·4 for O_2, 1·08 to 1·64 for CO_2, and 1·018 to 1·324 for Cl_2.

The asymptotic growth period is preceded by an early growth period of very short duration. During this first period, surface tension forces are significant. In Fig. 6 this period is practically zero. In Fig. 7 the early growth is complete in something like 0·0006 s, which is less than the time for one motion picture frame. The order of the early-growth rates does not correlate with the order of the current density. A possible explanation is given in the section, "Effect of electrode metal". The asymptotic growth, on the other hand, correlates well with current density, as described below.

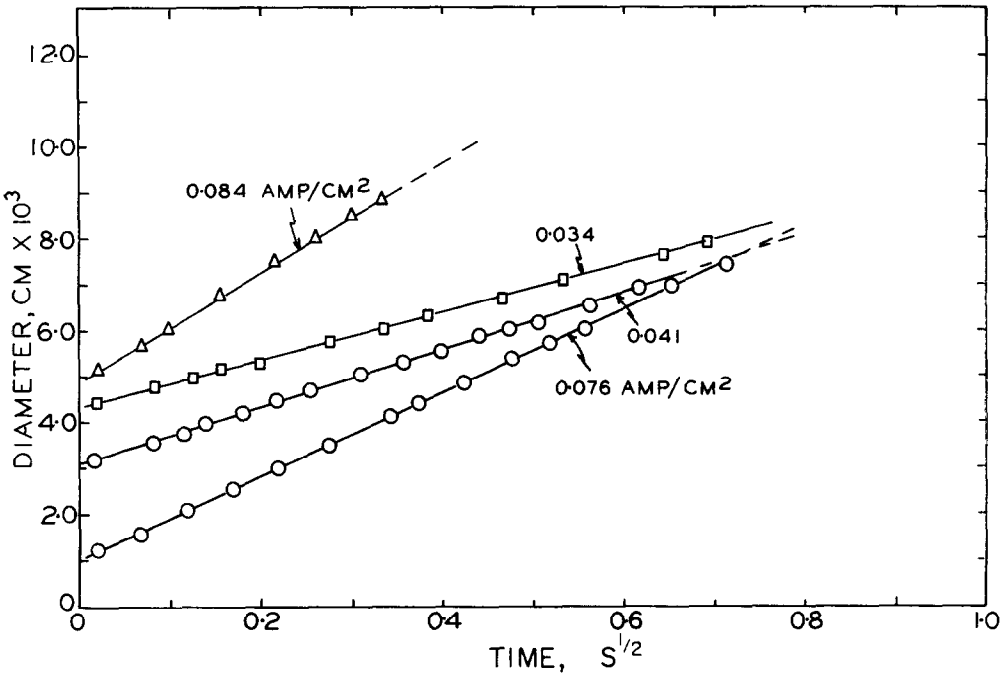

FIG. 7. Very rapid early growth in one movie frame followed by normal growth. H_2 on 4 different sites on 0·127 mm Ni cathode in 1·0 N H_2SO_4 at 1 atm.

Effect of current density

Tests were made with the current density varying from 0·01 to 0·12 A/cm². The bubble growth rates for all the gases and all the electrodes increased with increases in the electrical current. The theoretical growth equations, such as equations (2) to (5) do not contain current density. However, the local supersaturation and therefore the concentration driving force which is represented here by $C_\infty - C_s$ undoubtedly depend on the current density.

Two models are apparent for predicting how the growth coefficient β might depend on the current density I. For purposes of distinction here, they will be called the *steady-state* model and the *unsteady-state* model.

The simpler model is the *steady-state* one. This assumes that the rate of gas production in a bubble is proportional to the electrical current. This model cannot be exact, because in the real situation bubble production at any site is intermittent. Thus, local storage and depletion of solute occur continuously. However, according to the model, equations (7) and (8) result.

$$R = KI^{1/3} \tag{7}$$

$$\beta = K_1 I^{1/3} \tag{8}$$

Here K_1 is a proportionality constant which depends on the gas density, its valence, solubility, and perhaps other factors. In principle the numerical value of K_1 should be predictable from the elementary laws of electrochemistry; but in practice with the miniature electrode, the theoretical and empirical values for K_1 disagreed by much more than the magnitude of data scatter. This may be interpreted to mean that the solute supersaturation does not hold at a steady level as demanded by the steady-state model.

If equation (8) is to be useful, it must give a good correlation of data. An empirical value of K_1 may be selected for a particular system. This was done, and equation (8) is shown as a dashed line in Figs. 8 to 13. The correlation is good in general, and in some selected cases such as in Figs. 9(a) and 10(a), it is near perfect.

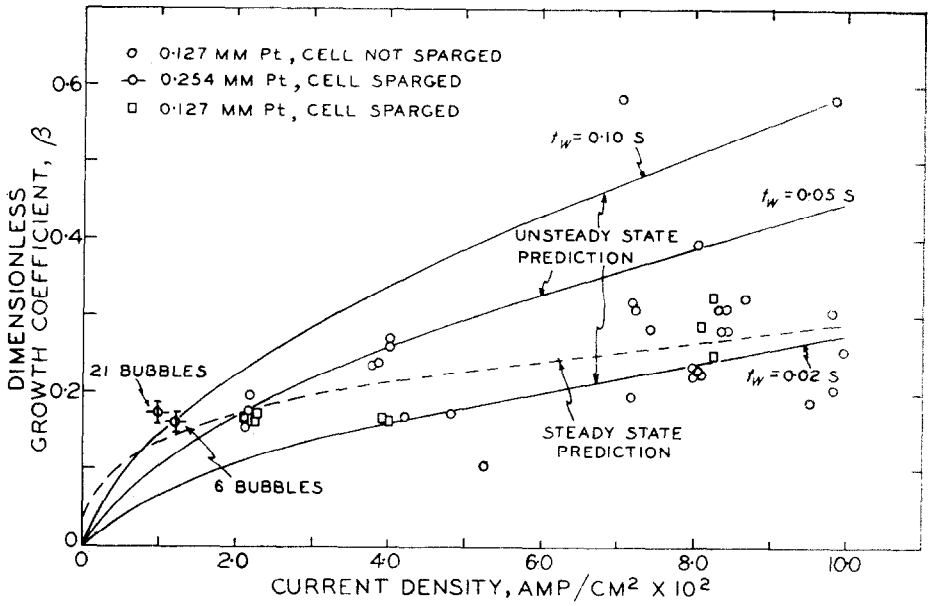

FIG. 8. Illustration of two theoretical models for effect of current density. Dashed line is equation (8), solid line is equation (9). H_2 on Pt in 1·0 N H_2SO_4 at 1 atm.

The other cases showed more data scatter, for reasons discussed later, or seemed to fit better to a second model.

The so-called *unsteady-state* model is a second mode for relating the growth coefficient to the current density. This was first proposed for the analogous heat-transfer problem by Hsu [17, 18] who considered bubble growth on a heated wall in a boiling liquid. The model requires a waiting time before a bubble can be born. During this waiting period the electrolysis continues in a steady manner and generates a flux of gas molecules which stay in solution. The supersaturation profile has a shape given by the error function [19]. The concentration everywhere increases until it reaches a critical value at a specific distance away from the electrode. For the boiling tests the critical distance is about 0·02 mm which is about the same as the size of a nucleation site.

For hydrogen bubbles with the present tests, the waiting time was usually much less than 1 s. Let us consider typical values of 0·02, 0·05, and 0·1 s. As a typical boundary-layer thickness let us use 0·01 mm. These values are arbitrary, but reasonable. Once the bubble nucleates, it is assumed then to grow with a constant driving force, $C_\infty - C_s$. In Fig. 8, the three solid curves show the resulting theoretical dependence of β on the current density. It is seen that these representations are sensible. In fact, this suggests that the data scatter is really a matter of different waiting times for different bubbles and of different boundary-layer thicknesses required for different nucleation sites.

Let us consider Scriven's equations for bubble growth. As Scriven points out, at low values of β a limiting solution results exactly in $\Phi = 2\beta^2$. In Fig. 1 it can be shown that for the range of data for electrolytic bubbles of hydrogen ($\beta = 0{\cdot}1$ to $0{\cdot}3$), a straightline fit gives $\Phi = 1{\cdot}07\ \beta^{1{\cdot}8}$, or $\beta \propto \Phi^{0{\cdot}55}$. But inasmuch as Φ is directly proportional to the mass diffusion rate, and the mass diffusion rate is proportional to the current density, the unsteady-state model for the electrolytic hydrogen bubbles may be expressed approximately by equation (9).

$$\beta = K_2 I^{0{\cdot}55} \tag{9}$$

Here K_2 is an empirical proportionality constant.

In Fig. 8, it is not easy to choose between the two theoretical models; this is because so many different nucleation sites were used that a sizeable scatter of data resulted. However, in Figs. 9(a) and 10(a), the data scatter is very small because just four nucleation sites were used in each figure. Equation (8) is definitely superior to equation (9) in these two graphs. Only equation (8) is shown in these graphs; it fits almost perfectly. Equation (9) can be made to fit the data at a current density of 0·04 A/cm^2, but the resulting curve is high in Figs. 9(a) and 10(a) by about 14 per cent at a current density of 0·08 A/cm^2. It is concluded that equation (8) is more reliable than equation (9) for H_2, and the steady-state model is preferred for relating the growth coefficient to the current density for H_2.

The value of the exponent (and the coefficient) in equation (9) is slightly different for the tests with O_2, CO_2, and Cl_2, because they cover a slightly different range of values of β in Fig. 1. Using for all these gases a power relationship, $\Phi = 0{\cdot}77\ \beta^{1{\cdot}66}$, which holds reasonably well over the range of values of β from 0·1 to 0·9, equation (10) results.

$$\beta = K_3 I^{0{\cdot}6} \tag{10}$$

Figure 11 shows data for O_2 compared to equations (8) and (10). Here equation (10) for the unsteady-state model is better. Figure 12 shows the comparison for Cl_2. Although equation (8) is better for the tests in the unsparged liquid (bulk undersaturated), equation (10) is better for Cl_2 in the sparged liquid (bulk saturated). Figure 13 shows the comparison between equations (8) and (10) for CO_2. For the sparged liquid, the two equations are of about equal satisfaction. The data scatter for the unsparged liquid is rather large and prevents a reliable comparison.

Apparently both models for correlating the effect of current density are useful. For H_2, the steady-state model is better; for O_2 and Cl_2, the

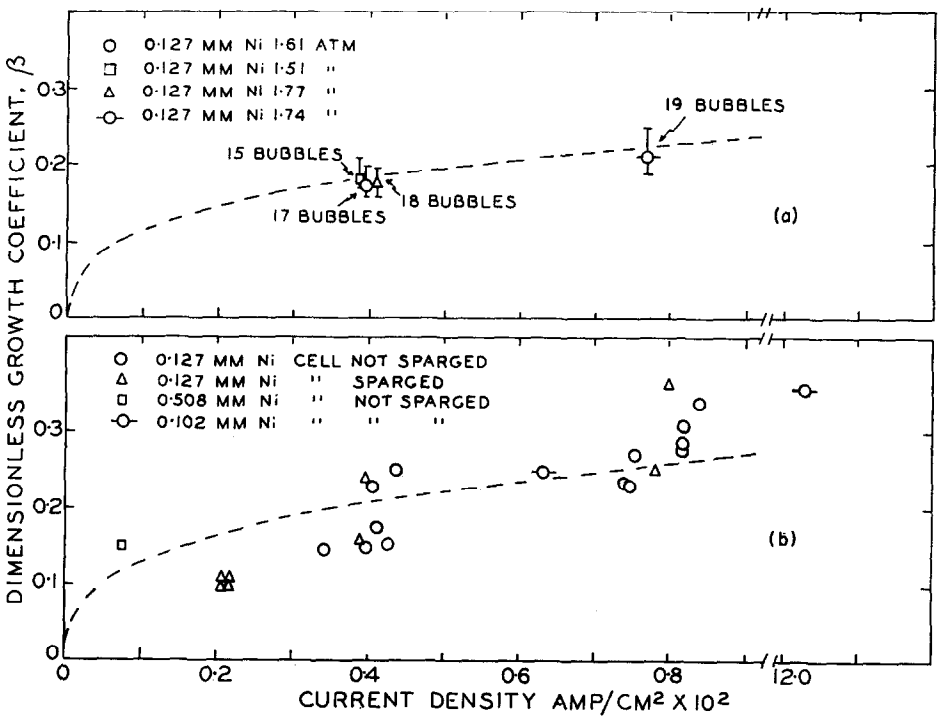

FIG. 9. Data for H_2 on Ni showing variability of nucleation sites. (a) Four sites only in use. (b) 24 sites in use. All tests in 1·0 N H_2SO_4. Dashed line is equation (8).

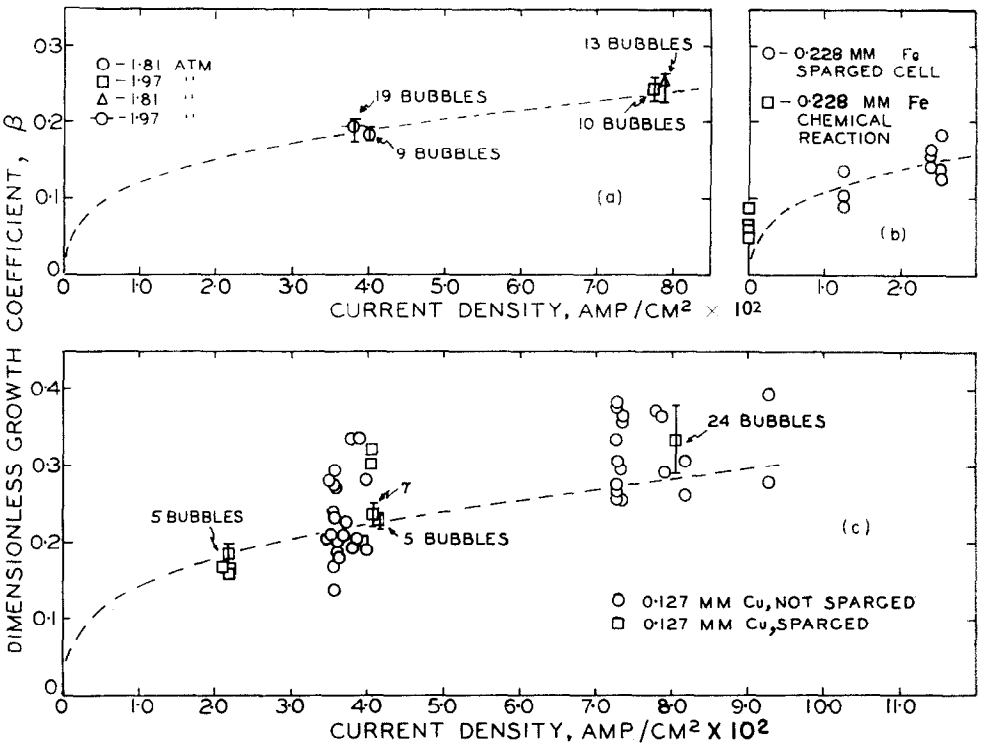

FIG. 10. Bubbles of H_2 in 0·10 H_2SO_4. (a) Four nucleation sites on Pt at elevated pressures. (b) Iron cathode shows bubble growth from chemical reaction at zero imposed current. (c) Copper cathode with 35 nucleation sites.

unsteady-state model is better; for CO_2 both are about of equal accuracy. Probably the real physical phenomenon lies somewhere between the two models.

Variation in nucleation sites

Figure 8 shows data obtained with about 40 different nucleation sites. These were microscopic pits and scratches such as observed by earlier workers [1, 5]. Other series of runs employing a different site for each bubble (with polishing being done between runs) are Figs. 9(b), 10(b), 11, and 13. In each of these graphs the data scatter is quite noticeable.

In contrast, all bubbles in Fig. 9(a) were grown on four nucleation sites. Note the distinct decrease in the scatter of data. Another example is Fig. 10(a). This demonstrates convincingly that the growth rate of an electrolytic bubble depends on the size, shape, or some other aspect of the nucleation site.

Even at a single site at constant test conditions, successive bubbles show some variability in growth behavior. For example, in Fig. 9(a) at 0·077 A/cm², 19 replicate bubbles are represented. The mean, maximum, and minimum values of β are indicated. The 19 values are distributed in a statistical manner. Such statistical behavior is well known for successive bubbles formed at single sites during nucleate boiling [9, 10]. The present study of electrolytic bubbles shows that the variability of bubbles from different sites is much greater than the variability of bubbles from one site. In all probability, this is true also for bubble growth during nucleate boiling.

Effect of electrode diameter

Figure 8 includes data for 0·127 and 0·254 mm

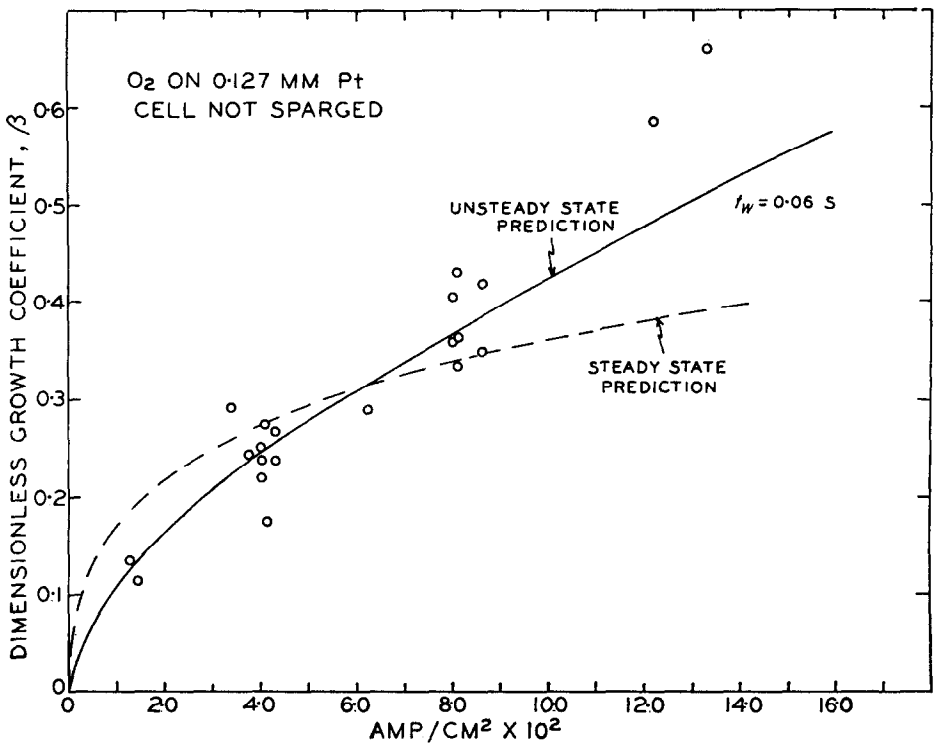

FIG. 11. Bubbles of O_2 at 1 atm in 0·1 and 1·0 N N_2SO_4; 0·1 and 1·0 N NaOH.

diameter electrodes. Figure 9(b) includes 0·102, 0·127, and 0·508 mm electrodes. Figure 14 includes 0·127 and 0·228 mm electrodes. Within this range of sizes, no effect on the growth coefficient was detected. If the electrode size does have an effect on bubble growth rates, it is a very weak variable.

Effect of electrode metal

Tests were made using four kinds of metal cathodes for H_2 bubbles. The decomposition voltage required in practice [20] to generate H_2 on platinum at an appreciable rate is 1·70 V. The reversible e.m.f. from thermodynamic free energy considerations is 1·23 V. The difference of 0·47 V is the overvoltage. Overvoltage depends on the metal and also on the current density. At 0·04 A/cm², it is 0·20, 0·65, 0·70, and 0·93 V for H_2 on Pt, Fe, Cu, and Ni, respectively. Figure 14(b) shows asymptotic growth data for H_2 on Pt, Cu, and Ni at 0·04 A/cm² and for Fe at 0·024 A/cm². Figure 14(a) shows data for Pt, Cu, and Ni at 0·08 A/cm². The abcissa is the overvoltage. Within the range studied, no effect can be detected. It must be emphasized that these tests were run with a controlled, constant current. If the tests had been conducted at constant voltage, the results could be quite different.

Although the asymptotic growth rate is independent of the metal, the very early growth which precedes the asymptotic period does depend on the metal. For example, nickel often resulted in very rapid early growth of H_2 bubbles for less than one movie frame (about 0·0006 s) as seen in Fig. 7 near zero time. Copper and platinum electrodes gave slower growing bubbles in this first-frame period, even at higher current densities. The apparent effect of metal on the very early growth might be a result of difference in nucleation sites. Nickel is a harder material than the other

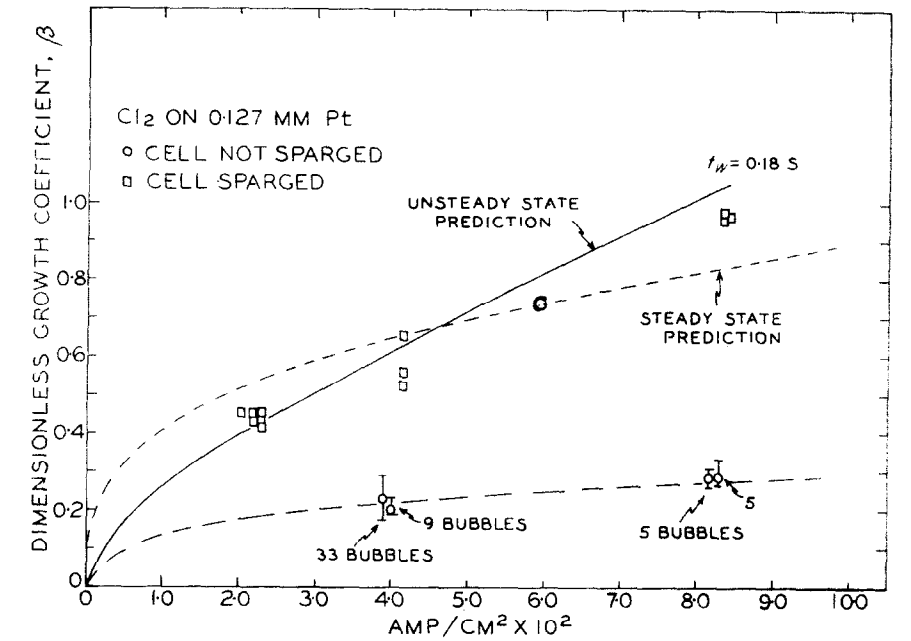

FIG. 12. Comparison of sparged and unsparged bulk liquid for electrolytic Cl_2 bubbles. 1 atm, in 1 N NaCl plus 0·01 N NaOH.

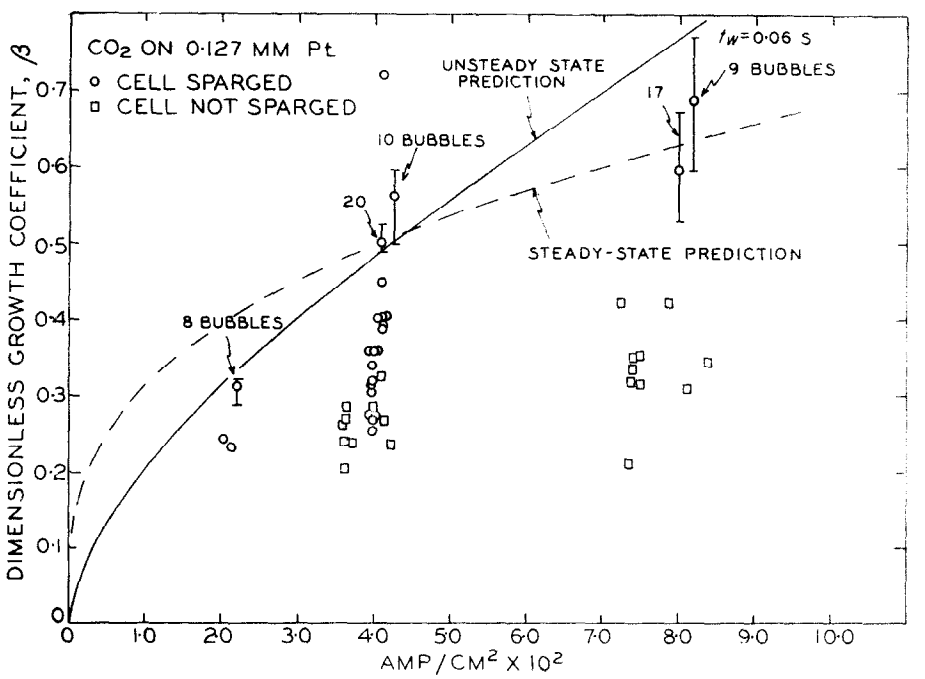

FIG. 13. Comparison of sparged and unsparged bulk liquid for electrolytic CO_2 bubbles. 1 atm, in 1·0 N $Na_2C_2O_4$ plus 30 wt per cent H_2SO_4.

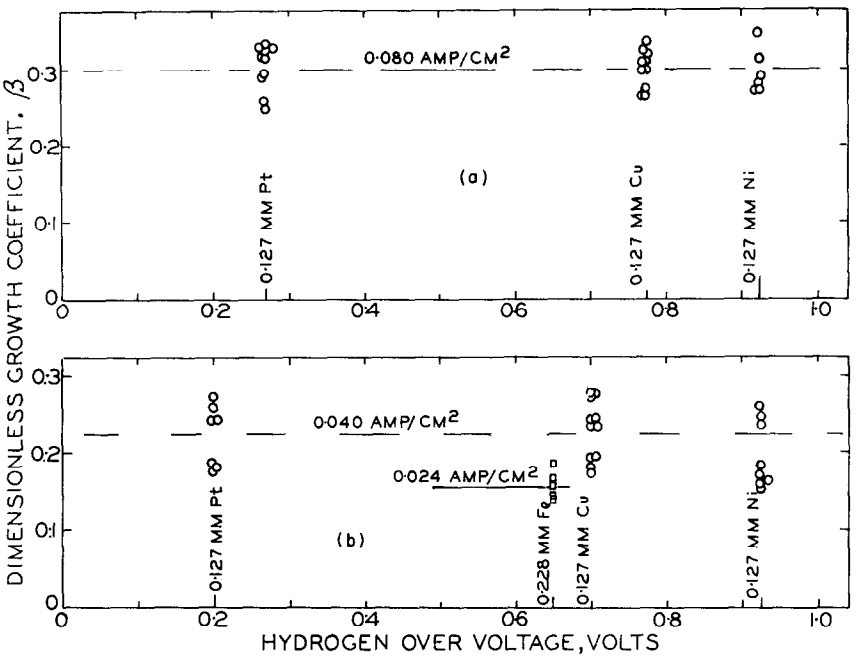

FIG. 14. Effect of electrode metal for H_2 in 1·0 N H_2SO_4 at 1 atm.

metals used. The tiny surface defects resulting from the polishing technique are probably different for hard and soft metals. Indeed the hardest material should have the smoothest polished surface. The exceedingly small size of the nucleation sites should result in unusually long waiting times. Such was observed. Waiting times with nickel were up to 30 s for H_2 at 0·04 A/cm², 5 min for O_2 and CO_2 at 0·08 A/cm², and 0·2 s for Cl_2 at 0·08 A/cm². Four tests only were made with Cl_2. For some tests with nickel anodes, the polished surface was scratched slightly, deliberately, with 2/0 emery paper just before use. This provided a few nucleation sites large enough to nucleate quickly. It is clear that long waiting times are associated with a lack of "large" nucleation sites, and that long waiting times lead to large local supersaturation which in turn causes very rapid early growth of bubbles for very short periods. A "large" nucleation site for electrolytic bubbles is something like 0·005 mm in size.

Effect of pressure

The parameter Φ, equation (4), contains two variables which are definitely pressure-dependent: the gas density ρ_G and the saturation concentration C_s. It seems evident that the supersaturation C_∞ must be a function of pressure also. For modest changes in pressure, ρ_G should vary according to Boyle's Law, and the concentrations should vary according to Henry's Law. Considering that $\rho_L \gg C_s$ for all tests herein, we conclude that modest changes in pressure should not affect Φ. Likewise, β should be unaffected

Data for tests with hydrogen at pressures from 1 to 2 atm are given in Figs. 8, 9, and 10. These and other tests are summarized in Fig. 15. It is concluded that pressure has no effect on the growth coefficient. If pressure is a variable, it is a very weak one.

Effect of contact angle

All the bubbles in this study were very small, and their shapes were spherical segments. The contact angle α, measured through the liquid, was computed readily using the bubble radius R and segment height h according to equation (11).

$$\cos \alpha = (h - R)/R \qquad (11)$$

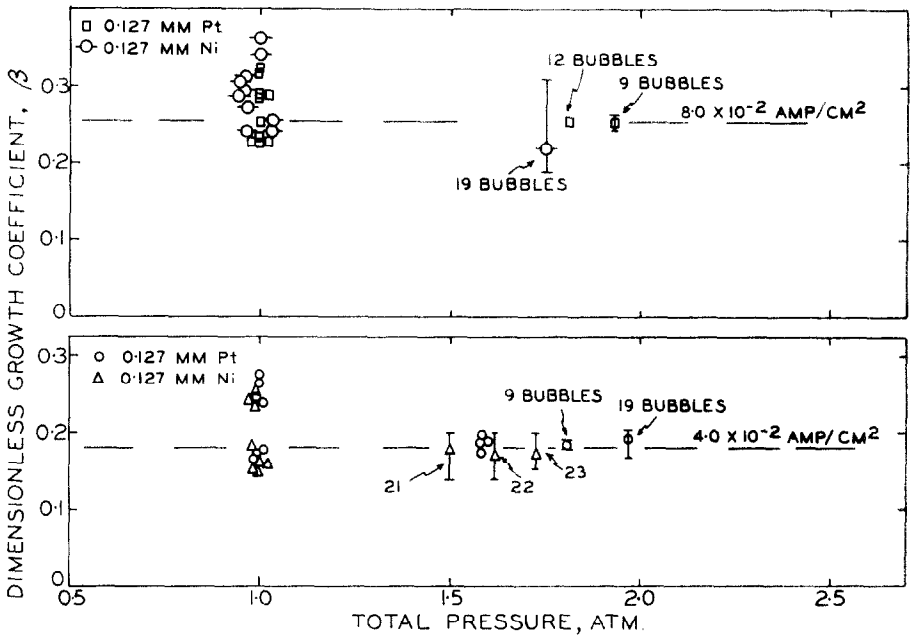

FIG. 15. Effect of pressure for H_2 bubbles in 0·1 N H_2SO_4.

The contact angle must have some effect on bubble growth for two reasons. For one, the liquid–gas interfacial area for a given volume of gas in the form of a spherical segment is a function of the contact angle as shown in Fig. 16. The area effect is seen to amount to no more than a 20 per cent change for all contact angles less than 150°. In the present study, no contact angle exceeded 100°, thus the area effect was not significant. The second reason concerns the movement of liquid solution which occurs as a bubble expands. Both factors were considered by Buehl and Westwater [8] in solving numerically for β vs. Φ for a spherical bubble tangent to a wall, shown as the upper line in Fig. 1. In the range of β values of interest here (0·1–0·9), the Buehl–Westwater values of β are about 18 per cent greater than the Scriven values. Therefore, the effect of contact angle was anticipated to be rather small.

Figure 17 shows how the contact angle changed during the growth of two typical bubbles, one of H_2 and one of CO_2. A striking fact is that the contact angle always changes during the growth of every electrolytic bubble. Any theoretical model for bubble growth that assumes a constant contact angle is incorrect in principle. In general, the angle decreases with increasing diameter, but many short-time exceptions were recorded. The base of the bubble frequently moved with a stick-and-slip behavior. In Fig. 17 the change in contact angle is large—from about 70 to 20°. This is almost enough to correspond to a shift from one curve to another in Fig. 1. For the CO_2 bubble the slope of the diameter vs. time line in Fig. 17 does indeed change by about this amount as the diameter increases. The change was not evident for the H_2 bubble.

It is concluded that contact angle has but a modest effect, of 20 per cent or less, on the growth coefficient for electrolytic bubbles with contact angles between zero and about 100°. This is expected from theory and is supported by data in Fig. 17 and by data for numerous other bubbles not shown here.

Physical properties

The four gases, four metals, different aqueous solutions, and the two-fold pressure

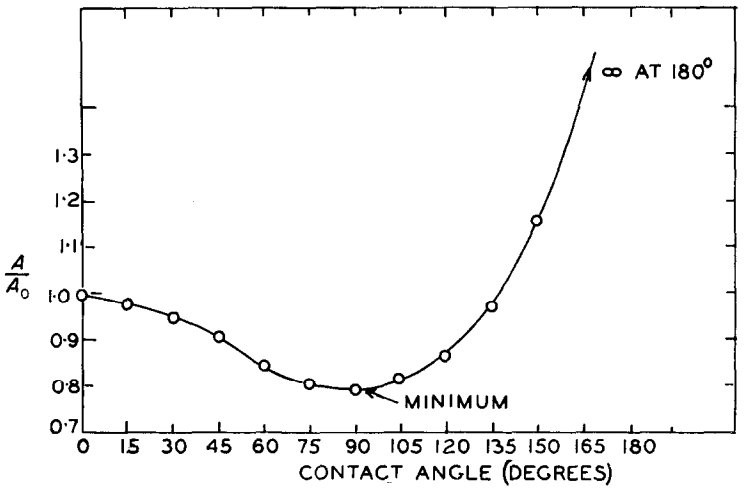

FIG. 16. Gas–liquid interfacial area for a spherical-segment bubble of constant volume on a solid wall.

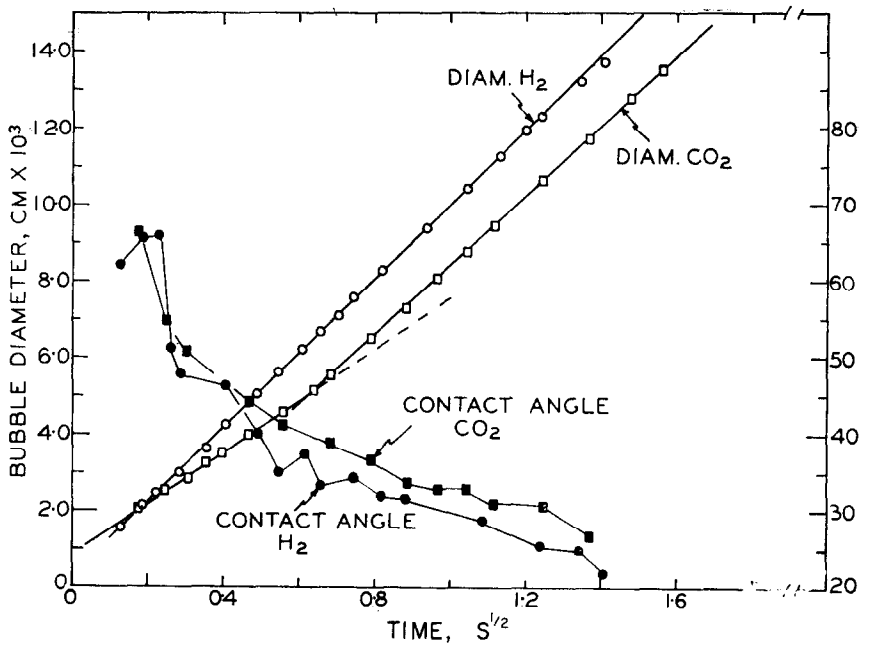

FIG. 17. Change of contact angle during bubble growth. H_2 on 0·127 mm Ni in 1·0 N H_2SO_4 at 0·041 A/cm²; CO_2 on 0·127 mm Pt in 1·0 N $Na_2C_2O_4$ with 30 wt per cent H_2SO_4 at 0·08 A/cm². 1 atm.

range provided a variety in the physical properties. The diffusivities at 28°C are $7{\cdot}38 \times 10^{-5}$ cm²/s for H_2, $2{\cdot}95 \times 10^{-5}$ for O_2, $2{\cdot}13 \times 10^{-5}$ for CO_2, and $1{\cdot}47 \times 10^{-5}$ for Cl_2. These values were taken from standard references [21, 22] and were adjusted for temperature by use of $D\mu/T = C'$ in a well-known manner [23]. The diffusivity in the solutions are assumed to be the same as in pure water. The values used for the saturation solubilities at 28°C are $0{\cdot}75 \times 10^{-6}$

mole/cm^3 for H_2, $1{\cdot}16 \times 10^{-6}$ for O_2, $30{\cdot}2 \times 10^{-6}$ for CO_2, and $85{\cdot}8 \times 10^{-6}$ for Cl_2. These also are for a pure water solvent [21, 24].

All the systems tested gave consistent behavior in that all could be described well by equation (2). The R vs $t^{1/2}$ fit for these tests at constant current density is better than for tests [1] at constant cell voltage. It is impossible at present to verify that either theoretical line in Fig. 1 is correct, because the supersaturation C_∞ cannot be measured by present techniques.

When CO_2 bubbles are grown in unsparged cells open to the room, the bubbles sometimes shrink after an initial growth and then resume growing. During the dissolving period the bulk solution must be undersaturated. When CO_2 bubbles are grown in an enclosed cell which is sparged with CO_2, no shrinkage occurs. Chlorine behaves similarly in sparged and unsparged cells. Figures 12 and 13 show slower bubble growth in unsparged cells than in sparged ones. Hydrogen shows no difference in growth in sparged and unsparged cells. Oxygen was run in unsparged cells only; presumably it would behave like H_2. Figures 8 to 10 show this result. The reason H_2 and O_2 need not be sparged is that the solubility is so small that a small flux of dissolved gas from the electrode is ample to saturate the liquid in a very short time. On the other hand, if a solution of CO_2 or Cl_2 is undersaturated, a relatively large amount of solute is needed to reach saturation. Put another way, it is easy to saturate water in an open cell with H_2 or O_2 produced at a small electrode. It is very difficult to saturate water in an open cell with CO_2 or Cl_2 produced at a small electrode.

Miscellaneous observations

Bubble coalescences and jump-off were observed in agreement with prior work [1]. An interesting, occasional observation was the ejection of a stream of bubbles from certain nucleation sites. This rapid-fire emission of a jet of bubbles occurred for H_2 on platinum cathodes and CO_2 on platinum anodes in 0·5 N and 1·0 N $Na_2C_2O_4$ electrolytes, but only when the metal had a relatively rough (2/0 emery paper) finish. Rapid-fire emission was reported earlier by Coehn and Neumann [3] for H_2 on platinum in 0·001 N H_2SO_4 in a strong electric field. It was called a "fountain effect" [4]. This type of bubble formation is desirable if it can be obtained on demand. It leads to rapid removal of gas from the electrode and a resulting low electrical resistance in the cell. It could not be obtained consistently in the present study. Figure 4 shows rapid emission.

The particular electrolyte selected seemed to have no effect for the present bubble growth studies. Note in Fig. 11 that O_2 was grown in both H_2SO_4 and NaOH solutions, with different normalities. No growth difference could be detected. Of course if liquids of extreme viscosity or density were used, the results might well be different.

A miscellaneous observation of interest concerns bubble growth of H_2 in 1·0 N H_2SO_4 on an iron cathode. Bubbles grew according to the square root of time relationship even when the imposed current was reduced to zero. This is indicated in Fig. 10(b). These bubbles were being produced, of course, by chemical attack (corrosion) on the electrode. These numbers are believed to be the only existing quantitative data for a 3-way phase change. In this case, liquid and solid disappeared as gas appeared.

ACKNOWLEDGEMENTS

Financial support was provided by the National Science Foundation. A Summer Fellowship was furnished by the Diamond Alkali Company. Considerable help was provided by H. F. Shirazi and J. D. Wagner.

REFERENCES

1. D. E. Westerheide and J. W. Westwater, Isothermal growth of hydrogen bubbles during electrolysis, *J. Amer. Inst. Chem. Engrs* **7**, 357–362 (1961).
2. L. E. Scriven, On the dynamics of phase growth, *Chem. Engng Sci.* **1**, 1–13 (1959).
3. A. Coehn and H. Neumann, Elektrostatische erscheinungen an elektrolytisch entwickelten gasblasen, *Z. Phys.* **20**, 54–81 (1923).
4. B. Kabanow and A. Frumkin, Über die grosse elektrolytisch entwickelter gasblasen, *Z. Phys. Chem.* **165**, 433–452 (1933).
5. Takao Murakawa, Points on the electrode surface where gas bubbles are most frequently formed during electrolysis, *J. Electrochem. Soc. Japan* **25**, No. 5, E-61-62 (1957).
6. G. Houghton, P. D. Ritchie and J. A. Thomson, The rate of diffusion of small stationary bubbles and the diffusion coefficients of gases in liquids, *Chem. Engng Sci.* **17**, 221–227 (1962).

7. R. H. DOREMUS, Diffusion of oxygen from contracting bubbles in molten glass. *J. American Ceramic Society* **43**, 655–661 (1960).
8. W. M. BUEHL and J. W. WESTWATER, Bubble growth by dissolution: influence of contact angle. Submitted to *J. Amer. Inst. Chem. Engrs.*
9. P. H. STRENGE, ALUF ORELL and J. W. WESTWATER, Microscopic study of bubble drowth during nucleate boiling. *J. Amer. Inst. Chem. Engrs* **7**, 578–583 (1961).
10. J. E. BENJAMIN and J. W. WESTWATER, Bubble growth in nucleate boiling of a binary mixture. *International Developments in Heat Transfer*, Proceedings of International Heat Transfer Conference, Boulder, Colorado, and London, 1961–62. A.S.M.E., 212–218 (1963).
11. LORD RAYLEIGH, On the pressure developed in a liquid during the collapse of a spherical cavity, *Phil. Mag.* **34**, 94–98 (1917).
12. P. S. EPSTEIN and M. S. PLESSET, On the stability of gas bubbles in liquid–gas solutions, *J. Chem. Physics* **18**, 1505–1509 (1950).
13. J. P. GLAS, Microscopic growth of electrolytic bubbles. Ph.D. Thesis, University of Illinois (1964).
14. D. N. CRAIG and J. I. HOFFMAN, Determination of the Faraday constant by the electrolytic oxidation of oxalate ions. *Electrochemical Constants*, U.S. Department of Commerce, National Bureau of Standards, Circular 524 (1953).
15. J. W. WESTWATER and D. E. WESTERHEIDE, Motion Picture, Growth of hydrogen bubbles during electrolysis. University of Illinois, Urbana, Illinois, 1960.
16. J. W. WESTWATER, Measurements of bubble growth during mass transfer. Chapter in *Cavitation in Real Liquids* (ed. by ROBERT DAVIES). Elsevier, Amsterdam (1964).
17. Y. Y. HSU and R. W. GRAHAM, An analytical and experimental study of the thermal boundary layer and ebullition cycle in nucleate boiling. Technical Note, *D*-594, National Aeronautics and Space Administration, Washington, D.C. (May, 1961).
18. Y. Y. HSU, On the size range of active nucleation cavities on a heating surface, *J. Heat Transfer* **84**, Ser. C, 207–216 (Aug., 1962).
19. H. S. CARSLAW and J. C. JAEGER, *Conduction of Heat in Solids*, p. 76. University Press, Oxford (1959).
20. C. L. MANTELL, *Electrochemical Engineering*, p. 53. McGraw-Hill, New York (1960).
21. J. H. PERRY (editor), *Chemical Engineer's Handbook*, p. 540. McGraw-Hill, New York (1960).
22. J. F. DAVIDSON, The determination of diffusion coefficients for sparingly soluble gases in liquids, *Trans. Inst. Chem. Engrs* **35**, 51–60 (1957).
23. R. B. BIRD, W. E. STEWART and E. N. LIGHTFOOT, *Transport Phenomena*, p. 513. Wiley, New York (1960).
24. *Handbook of Chemistry and Physics*, 38th Edition. Chemical Rubber, Cleveland (1956).

Résumé—Une étude expérimentale de la croissance de bulles pendant l'électrolyse a été conduite au moyen de la cinématographie ultrarapide à travers un microscope, Les bulles étaient des bulles de H_2, O_2, Cl_2 et CO_2 sur des électrodes de platine, de nickel, de cuivre et de fer, à des pressions de 1 à 2 atmosphères, avec des densités de courant constantes et contrôlées de 0,01 à 0,12 A/cm^2. On a trouvé que les vitesses de croissance asymptotique des bulles concordent avec les précisions théoriques de Scriven ou de Buehl et Westwater. Des 600 bulles observées, aucune ne croissait avec un angle de contact constant. Une conclusion d'importance pour les théoriciens est que l'angle de contact est précisément une variable très peu importante, au moins dans la gamme de 0 à environ 100 degrés.

Zusammenfassung—Mit Hilfe der Hochgeschwindigkeitsphotographie durch ein Mikroskop wurde eine experimentelle Untersuchung des Blasenwachstums bei der Elektrolyse durchgeführt. Die Blasen bestanden aus H_2, O_2, Cl_2 und CO_2 und entstanden an Elektroden aus Platin, Nickel, Kupfer und Eisen bei Drücken zwischen 1 und 2 atm und bei eingeregelten konstanten Stromdichten von 0,01 bis 0,12 A/cm^2. Es ergab sich ein asymptotisches Wachstum der Blasen, das mit der theoretischen Vorhersage von Scriven und der von Buehl und Westwater übereinstimmte. Von 600 beobachteten Blasen wuchs keine bei einem gleichbleibenden Randwinkel. Eine bedeutende Folgerung für theoretische Forscher ist deshalb, dass der Randwinkel tatsächlich eine ganz schwache Veränderliche bleibt, zumindest in dem Bereich von 0 bis ungefähr 100 Grad.

Аннотация—С помощью высокоскоростной киносъемки через микроскоп проводилось экспериментальное исследование роста пузырьков при электролизе. Исследовались пузырьки H_2, O_2, Cl_2 и CO_2 на платиновом, никелевом, медном и жедезном электродах при давлениях от 1 до 2 атм при регулируемых плотностях постоянного тока от 0,01 до 0,12 А/см^2. Установлено, что асимптотические скорости роста пузырьков согласуются с теоретическими расчетами как Скривена так Буэля и Уэсуотера. Было исследовано 600 пузырьков : ни один из них не рос при постоянном угле контакта. Можно сделать важный для теоретических исследований вывод о том, что угол контакта оказывает очень малое влияние, по крайней мере, при температурах от 0 до 100°.